MACHINE SCIENCE
ISSN: 2227-6912
E-ISSN: 2790-0479
2023, № 1 Pages 36 –45

MATHEMATICAL MODELS OF CUTTING FORCES IN TURNING OPERATIONS

Viktor GUZEEV[1], Igor DERYABIN[2], Dmitrii ARDASHEV[3*]

[1,2,3*]South Ural State University, Chelyabinsk, Russia

E-mail: guzeevvi@susu.ru[1], deriabinip@susu.ru[2], ardashevdv@susu.ru[3*]

Abstract: The paper considers a variant of the predictive determination of the cutting force components for non-free cutting when turning. It is established that both the process of plastic deformation and the process of friction on back surfaces adjacent to main and auxiliary cutting edges of the tool influence the magnitude and direction of a cutting force component. The resulting force is defined as the vector sum of the forces that occur on the main and auxiliary cutting edges. We propose to determine the cutting force direction in non-free cutting as a vector in the direction of chip flow relative to the main cutting edge. The cutting process photography fixes the inclination angle of the chip flow. It is confirmed that in free cutting, the direction of chip flow is perpendicular to the main cutting edge. Contour turning on CNC lathes is accompanied by a change in the direction of feed motion resulting in a change in the main and auxiliary kinematic angles of the cutting tool. An increase in the active length of the main cutting edge in this situation leads to an increase in the contact area of the back surface of the main cutting edge with the workpiece surface, and, consequently, to an increase in the friction component of force, acting on the main cutting edge. Experimental measurement of the cutting force components makes it possible to determine the degree of influence of the force components associated with both the process of plastic deformation of the work material and the process of friction on the back surfaces adjacent to the main and auxiliary cutting edges of the tool. The obtained analytical dependences express the functional relationship between the elements of the cutting modes, the geometric parameters of the cutters, the degree of wear, the shape of the workpiece surface, and physical and mechanical properties of the work material. A large set of parameters included in the formulas for determining the components of the cutting force allows adequate monitoring the nature of the force interaction of the elements in the technological system when processing parts.

Keywords: *cutting forces, contour turning, unstable force load on technological system*

Introduction.

Despite the short terms of technological preparation for multi-product manufacturing, technological solutions must ensure the accuracy of the manufactured parts and the specified productivity. The difficulty of fulfilling these parameters is often associated with such a feature of a technological system as the technological heredity of part errors from workpiece errors. The workpiece refinement factor is mainly determined by the magnitude of the forces acting in the cutting process and the stiffness of the technological system. Under these conditions, the predictive determination of cutting forces becomes a primary task in making technological decisions. When choosing a cutting tool and assigning cutting conditions, it is necessary to evaluate the workability of the workpiece material. Its value is related to cutting forces [1, 2]. When determining the optimal cutting conditions, one of the main limitations is the cutting forces [3, 4]. Experimental determination of cutting forces is very time-consuming [5 - 12]. Analytical models are of greater interest [13 - 16]. Many researchers have studied the effect of specific parameters of the cutting process on cutting forces [17 - 21]. To predict cutting forces when contour turning on CNC lathes, multifactor models are required that take into account variable cutting conditions.

Under the unsteady conditions, a significant part of the resulting errors is the dimension errors in the dynamic adjustment. To predict these errors, it is necessary to evaluate the cutting forces under conditions of multiaxis movement of the cutting tool. Cutting forces with sufficient practical accuracy can be determined based on considering the elementary components of the cutting force acting on an infinitely small section of the cutting tool edge. This approach makes it possible to build a universal mathematical model of the cutting force that is invariant to different types of processing [22].

Methods and results

Knowing the magnitude of the force acting on the elementary sections of the active part of the tool cutting edges, it is possible by integrating to determine the components of the cutting force for all processing conditions, both simple surfaces with generatrices located parallel to the machine coordinate axes and complex surfaces arbitrarily located in the machine coordinate system.

The magnitude and direction of the components of the cutting force that occurs during non-free cutting depends on the forces on the face and back surfaces of both the main and auxiliary cutting edges. The resulting force can be found as a vector sum of forces that occur on the main and auxiliary cutting edges.

$$\overline{P}_{xy} = \overline{P}^{main}_{xy(d)} + \overline{P}^{main}_{xy(fr)} + \overline{P}^{aux}_{xy(d)} + \overline{P}^{aux}_{xy(fr)}, \quad (1)$$

where $\overline{P}^{main}_{xy(d)}$ and $\overline{P}^{aux}_{xy(d)}$ are forces arising on the face surface of the main and auxiliary cutting edges; $\overline{P}^{main}_{xy(fr)}$ and $\overline{P}^{aux}_{xy(fr)}$ are forces arising on the back surface of the main and auxiliary cutting edges.

According to (1), the magnitude and direction of the cutting force radial-axial component depends on both the magnitude and the direction of the forces acting on the main and auxiliary cutting edges.

Let us analyze the significance of each of the components of (1) under the conditions of processing complex-profile surfaces with a variable direction of feed movement.

In the theory of metal cutting, there are no methods for analytically determining the influence of the feed movement direction on the direction of forces arising on the face surface of the main cutting edge, so this relationship was verified experimentally. Considering that the direction of the radial-axial component of the cutting force on the face surface of the cutter coincides with the direction of chip flow or differs from it by some constant value, the change in the direction of this force can be inferred by the direction of chip flow.

To fix the direction of chip flow during processing with different feed directions, we made experiments on photographing the cutting process. In order to eliminate the influence of forces on the auxiliary cutting edge on the direction of chip flow, processing was carried out under free cutting conditions. Measurements of chip flow angles along the face surface showed that the direction of chip flow does not change depending on the feed direction (Fig. 1).

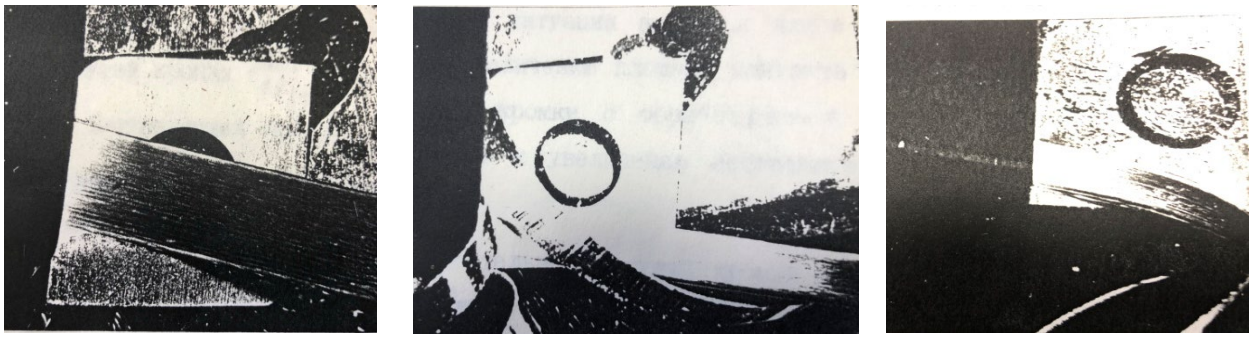

a) *b)* *c)*

Figure. 1. Photos of chip flow along the face surface in free cutting conditions at different inclination angles of the workpiece generatrix: a) ω =10° ; b) ω =30°; c) ω =60°.

Considering that the direction of the cutting force P_{xy} component is directly related to the direction of chip flow, we can conclude that the direction of the P_{xy} component in free cutting does not depend on the direction of feed movement. Therefore, a change in the direction of feed when turning a contoured surface does not cause an inclination of the axial P_x and radial P_y components of the cutting force in free cutting conditions.

When turning contoured surfaces with a constant contour feed, with a decrease in the main kinematic approach angle φ_κ, the width of cut increases, but at the same time, its thickness decreases. Calculations showed that when the angle of inclination of the workpiece surface changes from 0 to 90°, the cross-sectional area changes by no more than 5%. This change can be neglected and the area of the cut can be considered constant. From this, we can conclude that the magnitude of the force $\overline{P}^{main}_{xy(d)}$ also does not depend on the angle of inclination of the treated surface.

The active length of the main cutting edge, which increases in this case, leads to an increase in the contact area of the back surface of the main cutting edge with the surface to be machined, and, consequently, to an increase in the force component $\overline{P}^{main}_{xy(fr)}$.

To determine the degree of influence of the force $\overline{P}^{aux}_{xy(fr)}$ acting on the back surface of the auxiliary cutting edge on the change in the total radial-axial component of the force P_{xy}, experiments were carried out with the simultaneous photography of the chip flow (Fig. 2) and the dynamometry of the axial P_x and radial P_y components of the cutting force.

The hypothesis of the experiment was based on the fact that forces acting on the face surface of the tool determined the inclination angle of the chip from the normal to the cutting edge while the inclination angle η_r of the radial-axial component of the cutting force P_{xy} depended on both the forces acting on the face and back surfaces. Therefore, comparing the value of the inclination angle of the chip, measured from photographs of the cutting process, with the value of the inclination angle of the force calculated from the measured components P_x and P_y using the formula:

$$\rho = arctg\frac{P_y}{P_x} - (0{,}5\pi - \varphi)$$

we can conclude about the degree of $\overline{P}^{aux}_{xy(fr)}$ influence on the change of the P_{xy} component.

Table 1 shows the values of chip inclination angles obtained from photographs. Analyzing the obtained values of the angles, we see that the chip flows perpendicular to the diagonal of the cut layer. A number of researchers has already noted this fact.

Table 1.Values of chip inclination angles η_{ch}

φ_1, grad	3	9	15	30	45	60
η_{ch}, grad	8	8.2	8.6	9	9.2	10

Table 2 presents the values of P_x and P_y cutting force components measured at different auxiliary approach angles φ_1.

The calculated values of inclination angles of the P_{xy} force based on Table 2 are summarized in Table 3.

Table 2. Values of P_x and P_y components when machining 40X steel with cutters at different angles φ_1

φ_1, grad	3	9	15	30	45	60
P_x, N	469.5	394.2	340.5	322.5	308.2	274.1
P_y, N	178.0	282.0	242.6	224.1	199.5	168.8

Table 3. Inclination angles η_r of the force P_{xy} at different angles φ_1

φ_1, grad	3	9	15	30	45	60
η_r, grad	39.2	28.37	28.25	24.42	24.19	23.97

Comparing the angle values in Tables 1 and 2, we see that the inclination angles η_r of the force P_{xy} are much larger than the corresponding chip inclination angles η_{ch}. This proves that the forces on the back surface of the auxiliary cutting edge of the tool have a significant effect on the inclination of the radial-axial component of the cutting force P_{xy}.

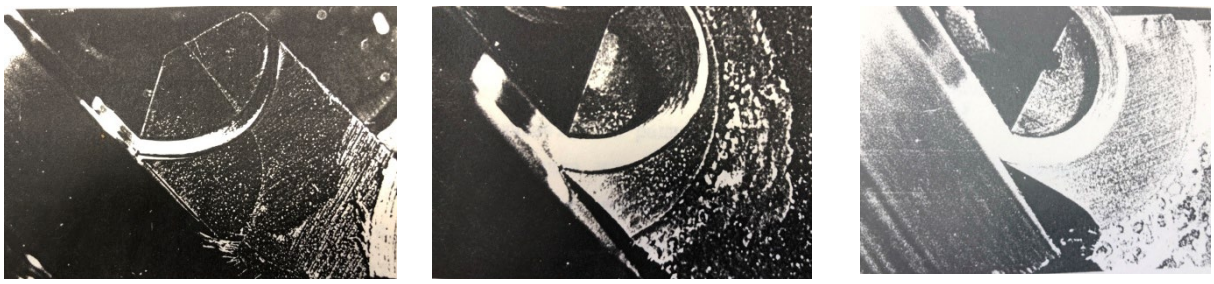

a) *b)* *c)*

Figure. 2. Photos of chip flow in non-free cutting conditions: a) φ_1 =3°; b) φ_1=15°; c) φ_1= 45°

Therefore, an increase in the auxiliary approach angle φ_1 leads to a decrease in the area of the cut by the auxiliary cutting edge and the area of the back surface contact with the workpiece. This causes a decrease in both components, $\overline{P}^{aux}_{xy(d)}$ and $\overline{P}^{aux}_{xy(fr)}$, of the cutting force on the auxiliary cutting edge.

The consequence of the change in forces on the auxiliary cutting edge is a change in the direction and magnitude of the P_{xy} component. Therefore, with an increase in the angle of inclination ω of the machined surface, the radial-axial component of P_{xy} can either increase if the force $\overline{P}^{main}_{xy(fr)}$ on the back surface of the main cutting edge has a dominant influence on its value, or decrease if the forces acting on the auxiliary cutting edge dominate. The radial-axial component of the cutting force P_{xy} is decomposed into radial P_y and axial P_x, which, therefore, also change during CNC contour turning. The nature of the change in P_x and P_y components depends on the static approach angles, φ and φ_1. Thus, if the main approach angle φ is less than or equal to 90°, P_x and P_y values are:

$$\overline{P}_x = \overline{P}^{main}_x - \overline{P}^{aux}_x;$$
$$\overline{P}_y = \overline{P}^{main}_y + \overline{P}^{aux}_y.$$

If the angle φ is more than 90°, P_x and P_y values are:

$$\overline{P}_x = \overline{P}^{main}_x + \overline{P}^{aux}_x;$$
$$\overline{P}_y = \overline{P}^{main}_y + \overline{P}^{aux}_y.$$

The components of the cutting force are determined in accordance with the options for forming the machined surface.

In the first case, when linear cutting edges make a stock removal and form residual irregularities, the cutting force components are found by integrating the expressions that determine the forces on the surface elements of the cutting edge. As a result,

$$P_{xy} = \left\{ [tg(\varphi-\eta)] \int_0^{S\cos\eta} \sigma_i в_{1i} \frac{\sin\beta}{\sqrt{3}\sin\beta_1\cos(\beta+\beta_1)} dв_1 + \right.$$

$$+ [tg(\varphi-\eta)+S\sin\eta] \int_{S\cos\eta}^{\frac{t\cos(\varphi-\eta)}{\sin\varphi}} \sigma_i в_{1i} \frac{\sin\beta}{\sqrt{3}\sin\beta_1\cos(\beta+\beta_1)} dв_1 +$$

$$\left. + [tg(\varphi-\eta)+tg(\varphi_1-\eta)] \int_{\frac{t\cos(\varphi-\eta)}{\sin\varphi}}^{в_1} \sigma_1(в_1-в_{1i}) \frac{\sin\beta}{\sqrt{3}\sin\beta_1\cos(\beta+\beta_1)} dв_1 \right\} +$$

$$+ 0{,}16\sigma_i \left[\frac{t(0{,}5\pi\rho+l_з)\cos(\varphi-\eta)}{\sin(\varphi\pm\omega)} + \frac{S(0{,}5\pi\rho+l'_з)\sin(\varphi\pm\omega)\cos(\varphi-\eta)}{\sin\varepsilon} \right], \qquad (2)$$

where $в_1$ is a conventional width of the removed layer [22].

$$P_z = \left\{ [tg(\varphi-\eta)] \int_0^{S\cos\eta} \sigma_i в_{1i} \frac{\cos\beta}{\sqrt{3}\sin\beta_1\cos(\beta+\beta_1)} dв_1 + \right.$$

$$+ [tg(\varphi-\eta)+S\sin\eta] \int_{S\cos\eta}^{\frac{t\cos(\varphi-\eta)}{\sin\varphi}} \sigma_i в_{1i} \frac{\cos\beta}{\sqrt{3}\sin\beta_1\cos(\beta+\beta_1)} dв_1 +$$

$$\left. + [tg(\varphi-\eta)+tg(\varphi_1-\eta)] \int_{\frac{t\cos(\varphi-\eta)}{\sin\varphi}}^{в_1} \sigma_1(в_1-в_{1i}) \frac{\cos\beta}{\sqrt{3}\sin\beta_1\cos(\beta+\beta_1)} dв_1 \right\} +$$

$$+ 0{,}16\sigma_i\mu \left[\frac{t(0{,}5\pi\rho+l_з)}{\sin(\varphi\pm\omega)} + \frac{S(0{,}5\pi\rho+l'_з)\sin(\varphi\pm\omega)}{\sin\varepsilon} \right]; \qquad (3)$$

P_x and P_y components for $\varphi \le 90^\circ$ are:

$$P_x = \sin\eta \left\{ \left[tg(\phi-\eta) \right] + tg\eta \int_0^{S\cos\eta} \sigma_i в_{1i} \frac{\sin\beta}{\sqrt{3}\sin\beta_1\cos(\beta+\beta_1)} dв_1 + \right.$$

$$\left. + \left[tg(\phi-\eta)+S\sin\eta \right] \int_{S\cos\eta}^{\frac{t\cos(\phi-\eta)}{\sin\phi}} \sigma_i в_{1i} \frac{\sin\beta}{\sqrt{3}\sin\beta_1\cos(\beta+\beta_1)} dв_1 + \right.$$

$$+\left[tg(\phi-\eta)+tg(\phi_1-\eta)\right]\int_{\frac{t\cos(\phi-\eta)}{\sin\phi}}^{в_1}\sigma_1(в_1-в_{1i})\frac{\sin\beta}{\sqrt{3}\sin\beta_1\cos(\beta+\beta_1)}dв_1\Bigg\}+$$

$$+0{,}16\sigma_i\left[\frac{t(0{,}5\pi\rho+l_з)\sin\phi}{\sin(\phi\pm\omega)}+\frac{S(0{,}5\pi\rho+l'_з)\sin(\phi\pm\omega)\sin\phi_1}{\sin\varepsilon}\right]; \quad (4)$$

$$P_y=\cos\eta\Bigg\{\left[tg(\varphi-\eta)\right]+tg\eta\int_0^{S\cos\eta}\sigma_i в_{1i}\frac{\sin\beta}{\sqrt{3}\sin\beta_1\cos(\beta+\beta_1)}dв_1+$$

$$+\left[tg(\varphi-\eta)+S\sin\eta\right]\int_{S\cos\eta}^{\frac{t\cos(\varphi-\eta)}{\sin\varphi}}\sigma_i в_{1i}\frac{\sin\beta}{\sqrt{3}\sin\beta_1\cos(\beta+\beta_1)}dв_1+$$

$$+\left[tg(\varphi-\eta)+tg(\varphi_1-\eta)\right]\int_{\frac{t\cos(\varphi-\eta)}{\sin\varphi}}^{в_1}\sigma_1(в_1-в_{1i})\frac{\sin\beta}{\sqrt{3}\sin\beta_1\cos(\beta+\beta_1)}dв_1\Bigg\}+$$

$$+0{,}16\sigma_i\left[\frac{t(0{,}5\pi\rho+l_з)\cos\varphi}{\sin(\varphi\pm\omega)}+\frac{S(0{,}5\pi\rho+l'_з)\sin(\varphi\pm\omega)\cos\varphi_1}{\sin\varepsilon}\right]. \quad (5)$$

In the second case, when the stock removal and the formation of residual irregularities are carried out by the radial part of cutting edges, the cutting force components are:

$$P_{xy}=\Bigg\{\int_{\frac{r-t}{r}\pm\omega}^{0{,}5\pi+\phi\pm\omega}r^2\left(1-\frac{1-t/r}{\sin\Theta_i}\right)\sigma_i\frac{\sin\beta\cos(\Theta_i+\eta-0{,}5\pi)}{\sqrt{3}\sin\beta_1\cos(\beta+\beta_1)}d\Theta_i+$$

$$+\int_{0{,}5\pi+\phi\pm\omega}^{\arccos(0{,}5S/r)\pm\omega}r-S\cos\Theta_i-\sqrt{r^2-S^2\sin^2\Theta_i}\,\frac{\sigma_i\sin\beta\cos(\Theta_i+\eta-0{,}5\pi)}{\sqrt{3}\sin\beta_1\cos(\beta+\beta_1)}d\Theta_i\Bigg\}+$$

$$+0{,}16\int_{\frac{r-t}{r}\pm\omega}^{\arccos(0{,}5S/r)\pm\omega}r(0{,}5\pi\rho+l_з)\sigma_i\left[0{,}5\pi-\arcsin(1-t/r)+,\right.$$

$$\left.+arctg(S/2r)\right]\cos(\Theta_i+\eta-0{,}5\pi)d\Theta_i, \quad (6)$$

where $\Phi = arctg\dfrac{\sqrt{r^2-(r-t)^2}-S}{r-t}$; Θ_i is the current angle of contact between the cutting edge and the workpiece.

In this case, the angle η, which determines the direction of the force P_{xy}, is determined as

$$\eta = arctg\frac{t-r+\left[r^2-(S/2)^2\right]^{0,5}}{\left[r^2-\left(r-t^2\right)\right]^{0,5}+\left\{r^2-\left[r^2-(S/2)^2\right]^{0,5}\right\}^{0,5}}.$$

$$P_z = \left\{\int_{\frac{r-t}{r}\pm\omega}^{0,5\pi+\phi\pm\omega} r^2\left(1-\frac{1-t/r}{\sin\Theta_i}\right)\sigma_i\frac{\cos\beta}{\sqrt{3}\sin\beta_1\cos(\beta+\beta_1)}d\Theta_i + \right.$$

$$\left. + \int_{0,5\pi+\phi\pm\omega}^{\arccos(0,5S/r)\pm\omega} r - S\cos\Theta_i - \sqrt{r^2-S^2\sin^2\Theta_i}\,\frac{\sigma_i\cos\beta}{\sqrt{3}\sin\beta_1\cos(\beta+\beta_1)}d\Theta_i\right\} +$$

$$+ 0{,}16r\mu(0{,}5\pi\rho + l_з)\sigma_i\left[0{,}5\pi - \arcsin(1-t/r+arctg(S/2r))\right] \quad . \qquad (7)$$

In the third case, when the radius and linear parts of the main cutting edge perform the stock removal, and the radial parts of the cutting edges form residual irregularities, the cutting force components are determined from the expressions:

$$P_{xy} = \left\{[tg(\varphi\pm\omega)] + tg\eta\int_0^{S\cos(\varphi-\eta)}\sigma_i\varepsilon_{1i}\frac{\sin\beta\cos(\varphi-\eta)}{\sqrt{3}\sin\beta_1\cos(\beta+\beta_1)}d\varepsilon_1 + \right.$$

$$+ \left[tS - S^2\sin(\varphi\pm\omega)\cos(\varphi\pm\omega)\right]\sigma_i\frac{\sin\beta\cos(\varphi-\eta)}{\sqrt{3}\sin\beta_1\cos(\beta+\beta_1)} +$$

$$\left. + \int_{0,5\pi+(\varphi\pm\omega)}^{H\pm\omega} r - \frac{r-S\sin(\varphi\pm\omega)}{\cos\Theta_i}\frac{\sigma_1\sin\beta\cos(\Theta_i-\eta-0{,}5\pi)}{\sqrt{3}\sin\beta_1\cos(\beta+\beta_1)}d\Theta_i\right\} +$$

$$+ \int_{H\pm\omega}^{\arccos(0,5S/r)\pm\omega} r - S\cos\Theta_i - \sqrt{r^2-S^2\sin^2\Theta_i}\,\frac{\sigma_1\sin\beta\cos(\Theta_i-\eta-0{,}5\pi)}{\sqrt{3}\sin\beta_1\cos(\beta+\beta_1)}d\Theta_i$$

$$+ 0{,}16\sigma_i(0{,}5\pi\rho + l_з)\left[\frac{t-r(1-\cos(\varphi\pm\omega))\cos(\varphi-\eta)}{\cos(\varphi\pm\omega)} + \right.$$

$$\left. + r(0{,}5\pi - \arccos(0{,}5S/r))\right]\cos(\varphi-\eta) \quad . \qquad (8)$$

$$P_z = \left\{ [tg(\varphi \pm \omega)] \int_0^{S\cos(\varphi - \eta)} \sigma_i в_{1i} \frac{\cos\beta}{\sqrt{3}\sin\beta_1 \cos(\beta + \beta_1)} d в_1 + \right.$$

$$+ \left[tS - S^2 \sin(\varphi \pm \omega)\cos(\varphi \pm \omega) \right] \sigma_i \frac{\cos\beta}{\sqrt{3}\sin\beta_1 \cos(\beta + \beta_1)} +$$

$$\left. + \int_{0,5\pi + (\varphi \pm \omega)}^{H \pm \omega} r - \frac{r - S\sin(\varphi \pm \omega)}{\cos\Theta_i} \frac{\sigma_1 \cos\beta}{\sqrt{3}\sin\beta_1 \cos(\beta + \beta_1)} d\Theta_i \right\} +$$

$$+ \int_{H \pm \omega}^{\arccos(0,5S/r) \pm \omega} r - S\cos\Theta_i - \sqrt{r^2 - S^2 \sin^2\Theta_i} \frac{\sigma_1 \cos\beta}{\sqrt{3}\sin\beta_1 \cos(\beta + \beta_1)} d\Theta_i +$$

$$+ 0,16\sigma_i \mu (0,5\pi\rho + l_з) \left[\frac{t - r(1 - \cos(\varphi \pm \omega))\cos(\varphi - \eta)}{\cos(\varphi \pm \omega)} + r(0,5\pi - \arccos(0,5S/r)) \right]. \quad (9)$$

In (8) and (9), the variable H is

$$H = -arctg \frac{r\cos(\varphi \pm \omega)}{r\sin(\varphi \pm \omega) - S}.$$

The angle η in this case is

$$\eta = arctg \frac{t - r + \left[r^2 - (S/2)^2 \right]^{0,5}}{t - r(1 - \cos\varphi)ctg\varphi + r\sin\varphi + S/2}.$$

It is possible to determine the components P_x and P_y from the known relations:

$$P_x = P_{xy} \sin\eta;$$
$$P_y = P_{xy} \cos\eta.$$

Conclusion. The resulting analytical dependencies express the functional relationship between the elements of cutting modes (feed and depth of cut), the geometric parameters of the cutters (approach angles φ and φ_1, and tip radius r), the degree of wear (l_w and ρ), the shape of the machined surface (ω), which also affects the position and length of the active parts of the cutting edges of the cutter ($в$), and physical and mechanical properties of the work material (σ_i). A large set of parameters included in the formulas for determining the components of the cutting force allows adequate monitoring the nature of the force interaction of the technological system elements when processing parts.

The calculation of cutting forces according to the developed formulas shows that when the inclination angle of the machined surface changes from +50° to –40° (which corresponds to the real conditions for processing complex surfaces), the radial component P_y of the cutting force changes by 4 times, and the axial component P_x changes by 200 times. Such significant changes in the components of the cutting force cause instability in the force load on the technological system and generate elastic displacements of its elements, which in turn increases the cutting inaccuracies.

REFERENCES

[1]. Vaxevanidis N.M., Kechagias J.D., Fountas N.A., Manolakos D.E. *Evaluation of Machinability in Turning of Engineering Alloys by Applying Artificial Neural Networks.* The Open Construction and Building Technology Journal. Vol., 2015, 8(1), pp. 389-399. DOI:10.2174/1874836801408010389

[2]. Al-Ahmari A.M.A. *Predictive machinability models for a selected hard material in turning operations.* Journal of Materials Processing Technology, 2007, vol. 190(1), pp. 305-311.

[3]. Aouici H., Yallese M.A., Chaoui K., Mabrouki T., Rigal J.F. *Analysis of surface roughness and cutting force components in hard turning with CBN tool: Prediction model and cutting conditions optimization.* Measurement, 2012, vol. 45(3), pp. 344-353.

[4]. Chua M.S., Rahman M., Wong Y.S., Loh H.T. *Determination of optimal cutting conditions using design of experiments and optimization techniques.* International Journal of Machine Tools and and Manufacture, 1993, vol. 33(2), pp. 297-305.

[5]. Lapshin V.P., Turkin I.A., Khristoforova V.V. *Assessment of Metal Wear in Turning on the Basis of Components of the Cutting Force.* Russ. Engin. Res., vol. 40, pp. 797–800 (2020). https://doi.org/10.3103/S1068798X20090099

[6]. Vaxevanidis N.M., Fountas N.A., Kechagias J., Malonakos D.E. *Estimation of Main Cutting Force and Mean Surface Roughness in Turning of AISI D6 Tool Steel using Design of Experiments and Artificial Neural Networks.* In book MACHINING: Operations, technology and management, Nova Publishers, 2013, pp. 159-187.

[7]. Hwang Y.K., Lee C.M. *Surface roughness and cutting force prediction in MQL and wet turning process of AISI 1045 using design of experiments.* Journal of Mechanical Science and Technology, 2010, vol. 24(8), pp. 1669-1677.

[8]. Sieben B., Wagner T., Biermann D. *Empirical modeling of hard turning of AISI 6150 steel using design and analysis of computer experiments.* Production Engineering, 2010, vol. 4(2-3), pp. 115-125.

[9]. Youssef Y.A., Beauchamp Y., *Thomas M. Comparison of a full factorial experiment to fractional and Taguchi designs in a lathe dry turning operation.* Computers & industrial engineering, 1994, vol. 27(1-4), pp. 59-62.

[10]. Tan L., Chen Z., Huang J., et al. *Empirical models for cutting forces in finish dry hard turning of hardened tool steel at different hardness levels.* Int. J. Adv. Manuf. Technol., 2014, vol.76, pp. 691–703. https://doi.org/10.1007/s00170-014-6291-8

[11]. Orra K., Choudhury S.K. *Mechanistic modelling for predicting cutting forces in machining considering effect of tool nose radius on chip formation and tool wear land.* Int. J. Mech. Sci., 2018, vol. 142–143, pp. 255–268. https://doi.org/10.1016/j.ijmecsci.2018.05.004

[12]. Campocasso S., Poulachon G., Costes J.P., Bissey-Breton S. *An innovative experimental study of corner radius effect on cutting forces.* CIRP Ann. Manuf. Technol, 2014, vol. 63, pp. 121–124. https://doi.org/10.1016/j.cirp.2014.03.076

[13]. Imani B.M., Yussefian N.Z. *Cutting force simulation of machining with nose radius tools.* IEEE. International Conference on Smart Manufacturing Application, 2008, pp. 19–23.

[14]. Arsecularatne J.A., Mathew P., Oxley P.L.B. *Prediction of chip flow direction and cutting forces in oblique machining with nose radius tools*. Proc. Inst. Mech. Eng. Part B J. Eng. Manuf., 1995, vol. 209, pp. 305–315. https://doi.org/10.1243/PIMEPROC_1995_209_087_02

[15]. Abdellaoui L., Bouzid W. *Thermomechanical approach for the modeling of oblique machining with a single cutting edge.* Mach. Sci. Technol, 2016, vol. 20, pp. 655–680. https://doi.org/10.1080/10910344.2016.1224020

[16]. Abdellaoui L., Bouzid W. *Thermomechanical modeling of oblique turning in relation to tool-nose radius.* Mach. Sci. Technol, 2016, vol. 20, pp. 586–614. DOI:10.1080/10910344.2016.1224017.

[17]. Özel T., Hsu T.K., Zeren E. *Effects of cutting edge geometry, workpiece hardness, feed rate and cutting speed on surface roughness and forces in finish turning of hardened AISI H13 steel.* The International Journal of Advanced Manufacturing Technology, 2005, vol. 25 (3-4), pp. 262-269.

[18]. Endres W.J., Kountanya R.K. *The effects of corner radius and edge radius on tool flank wear.* J. Manuf. Process, 2002, vol. 4, pp. 89–96. https://doi.org/10.1016/S1526-6125(02)70135-7

[19]. Bartarya G., Choudhury S. K. *Effect of cutting parameters on cutting force and surface roughness during finish hard turning AISI52100 grade steel.* Procedia CIRP, vol. 1, pp. 651-656 (2012).

[20]. Meyer R., Köhler J., Denkena B. *Influence of the tool corner radius on the tool wear and process forces during hard turning.* Int. J. Adv. Manuf. Technol, 2012, vol. 58, pp. 933–940. https://doi.org/10.1007/s00170-011-3451-y

[21]. Childs T.H.C., Sekiya K., Tezuka R., et al. *Surface finishes from turning and facing with round nosed tools.* CIRP Ann, 2008, vol. 57, pp. 89–92. https://doi.org/10.1016/j.cirp.2008.03.121

[22]. Guzeev V.I. *Improving the efficiency of integrated technological processes at the stages of design and implementation.* (in Russ). Science-intensive technologies in mechanical engineering, 2014, No. 7 (37). pp. 36-41.

Received: 14.03.2023
Accepted: 16.05.2023